Characterization of grain boundary impedances in fine- and coarse-grained $CaCu_3Ti_4O_{12}$ ceramics

Timothy B. Adams, Derek C. Sinclair, and Anthony R. West
University of Sheffield, Department of Engineering Materials, Sir Robert Hadfield Building, Mappin Street, Sheffield, S1 3JD, United Kingdom

(Received 25 November 2005; revised manuscript received 17 January 2006; published 28 March 2006)

The influence of electrode material, dc bias, and pellet thickness on the electrical properties of fine- and coarse-grained $CaCu_3Ti_4O_{12}$ (CCTO) ceramics has been investigated using impedance spectroscopy. The low frequency arc observed in Z^* plots near room temperature is independent of the electron work function of the metal electrode. It shows significant variation with dc bias and pellet thickness for coarse-grained ceramics, but no such variations for fine-grained ceramics. The results demonstrate the importance of ceramic microstructure in controlling the electrical properties of CCTO ceramics and support the internal barrier layer capacitor (IBLC) model of Schottky barriers at the grain boundaries between semiconducting grains. The IBLC model explains the high permittivity and nonlinear current-voltage characteristics commonly reported for CCTO ceramics.

DOI: 10.1103/PhysRevB.73.094124 PACS number(s): 77.22.Ch, 77.22.Gm

I. INTRODUCTION

$CaCu_3Ti_4O_{12}$ (CCTO) is one of a family of phases with a perovskite-related structure (general formula ABO_3) in which Ca^{2+} and Cu^{2+} ions share the A site.[1] The size difference between Ca^{2+} and Cu^{2+}, and their ordered occupation of the A site, causes the TiO_6 octahedra to undergo substantial tilting ($a^+a^+a^+$ in Glazer's notation[2]), leading to a body-centered cubic supercell of space group $Im3$ in which the Ti^{4+} ions occupy the centrosymmetric position in the octahedral sites. The angle of tilt is sufficiently large that the Cu^{2+} ions occupy an essentially square-planar environment. To date, no structural phase transitions have been reported for CCTO in the range 37–1000 K.[3]

Many phases isostructural with CCTO were discovered throughout the late 1960s and during the 1970s; however, investigation into their electrical properties began only recently. In 2000, Subramanian *et al.*[4] reported a high permittivity of ~12,000 in CCTO ceramics which, when measured at 1 kHz, remained constant between room temperature (RT) and ~300 °C; the authors also reported a decrease in the RT permittivity with increasing measuring frequency. It was suggested that this behavior was either an intrinsic property associated with some form of ferroelectric relaxation involving displacement of the Ti^{4+} ions or an extrinsic effect associated with electrical heterogeneities, such as insulating grain boundary layers between semiconducting grains, as found in $SrTiO_3$-based internal barrier layer capacitors (IBLCs) and ZnO-based varistors. In the latter case, the 'effective' permittivity from an IBLC-type device can be estimated as $\varepsilon_{\text{eff}} \sim \varepsilon_r(t_b/t_{\text{gb}})$ where ε_r is the relative permittivity of the insulating grain boundary phase, t_b is the average grain size and t_{gb} is the average thickness of the grain boundaries.

Since the original report by Subramanian *et al.*, there has been substantial debate about the intrinsic and extrinsic electrical properties of CCTO. This has arisen due to various groups performing different types of experiment on a variety of forms of CCTO, i.e, single crystals, films and ceramics. For example, Holmes *et al.*[5] and Ramirez *et al.*[6] measured permittivity and tan δ of single crystals of CCTO at selected frequencies between 20 Hz and 1 MHz from RT to ~4 K. When measured at 20 Hz, a permittivity of ~350 000 was observed, which dropped to ~100 upon cooling to below 75 K, coinciding with a peak in tan δ. Measuring at higher frequencies appeared to increase the so-called "transition temperature." They suggested that the high permittivity originated from an exotic polarization mechanism facilitated by the CCTO structure, and that the transition to a low permittivity state was caused by "freezing" of dipole moments, thought to be associated with the Ti^{4+} ions; however, such an explanation was not consistent with the crystallographic information which shows no evidence of a structural phase transition or significant displacement of Ti^{4+} ions from the center of symmetry within the octahedral sites.

Sinclair *et al.*[7] used impedance spectroscopy (IS) to demonstrate that CCTO ceramics were electrically heterogeneous, consisting of semiconducting grains (with permittivity <100) and insulating grain boundaries. The data were analyzed using a simplified equivalent circuit consisting of two parallel RC elements connected in series, one RC element, R_bC_b, representing the semiconducting grains and the other, $R_{\text{gb}}C_{\text{gb}}$, representing the insulating grain boundary regions, Fig. 1(a). A schematic diagram of a typical impedance complex plane, Z^*, plot obtained at room temperature for CCTO ceramics is shown in Fig. 1(b). Based on this equivalent circuit, and in accordance with the brickwork layer model for electroceramics, the large arc observed at lower frequencies was attributed to the grain boundary response and the nonzero intercept on the Z' axis at high frequencies was attributed to the bulk resistance, R_b. Variable temperature measurements were performed and the activation energies for conduction associated with the bulk and grain boundary responses were found to be ~0.08(2) and 0.60(2) eV, respectively. This study supported the "extrinsic" IBLC model as the origin of the high permittivity in CCTO and also reconciled the 'intrinsic' properties of CCTO, i.e., a permittivity of

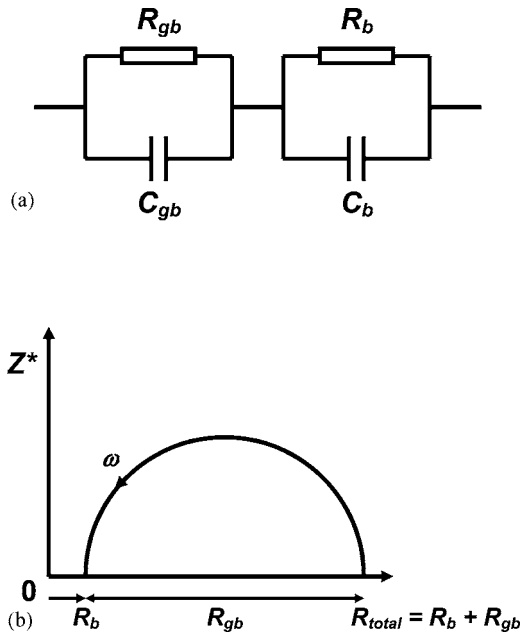

FIG. 1. Equivalent circuit (a) and schematic Z^* plot (b) for CCTO ceramics.

<100 is consistent with a tilted, centrosymmetric perovskite with only electronic and ionic polarizability mechanisms contributing to the permittivity. Adams, Sinclair, and West[8] subsequently used IS to show the influence of average grain size on the electrical properties of CCTO ceramics, reporting extremely high grain boundary capacitance ($\sim 10^{-8}$ F cm^{-1}) and effective permittivity values ($\sim$280 000 at 300 K) for large grained ($\sim$100–300 μm) ceramics, providing further support for the IBLC mechanism in CCTO ceramics. This IBLC model has been supported by other workers.[9,10]

Recently, Chung *et al.*[9] used a combination of scanning Kelvin probe microscopy with a lateral bias and *I-V* measurements on pellets and across individual grain boundaries (using microcontact electrodes on individual grains) to demonstrate the presence of electrostatic barriers at the grain boundaries in CCTO ceramics. The *I-V* characteristics of the ceramics and across single grain boundaries were nonlinear and consistent with that expected for Schottky-type barriers. Furthermore, they demonstrated that the breakdown voltage varied with the average grain size [$\sim$1300 and 300 V cm^{-1} for fine-grained (<5 μm) and large-grained ($\sim$50 μm) ceramics, respectively]. The grain size-dependent breakdown voltage supports the IBLC mechanism. From single grain boundaries on measurements across large grains, the threshold breakdown voltage was estimated to be $\sim$2.2 V/grain boundary. Chung *et al.*[9] concluded that fine-grained CCTO ceramics can be considered for applications as varistors as they have nonlinear (α) coefficients of $\sim$900 which far exceed the values, 30–80, of commercially available ZnO-based varistors.

Very recently, however, Lunkenheimer *et al.*[11] claimed that the high permittivity is associated with electrode polarization effects and the development of Schottky barriers at the metal electrode/ceramic interface due to nonohmic contacts and is not due to a grain boundary effect. Such nonohmic electrode contacts are wellknown to occur with many different types of materials, for example, in positive temperature coefficient of resistance (ptcr)-$BaTiO_3$ ceramics with Au electrodes, but can be eliminated by using an electrode material with a lower electron work function such as In-Ga alloy. Lunkenheimer *et al.* performed measurements using brass, Ag and Au electrodes and also measured ceramics with two different thicknesses (0.69 and 0.24 mm). The changes in permittivity observed below $\sim$1 MHz for both the electrode-type and pellet-thickness experiments were attributed to an electrode effect. In particular, the IBLC mechanism was ruled out on the basis that for it, the electrical properties should be independent of pellet thickness. Although this assumption is likely to be valid for fine-grained ceramics (at least for a "lower" pellet thickness of $\sim$0.24 mm) it may not be valid for coarse-grained ceramics, as described in the next section. Unfortunately, Lunkenheimer *et al.*[11] did not report any details on the microstructure of their ceramics and therefore, the assumption regarding the thickness experiment may or may not be valid.

In this paper, the influence of electrode material, dc bias and pellet thickness on the IS response of fine- and coarse-grained CCTO ceramics is reported. This allows discrimination of the grain boundary response from any significant electrode contact phenomenon. It confirms the Schottky-type nature of the electrostatic barriers at the grain boundaries and shows the electrical properties of fine-grained CCTO ceramics to be independent of pellet thickness (at least down to $\sim$0.4 mm). By contrast, coarse-grained ceramics show a dramatic variation in electrical properties as a function of pellet thickness. Prior to describing the results, a brief review of the influence of dc bias and ceramic microstructure on the electrical properties of Schottky-type grain boundary impedances in ceramics is provided.

II. SCHOTTKY BARRIERS

Schottky barriers are created in many commercial electroceramics such as ptcr $BaTiO_3$ thermistors and ZnO varistors by deliberate introduction of compositional heterogeneity between the grain and grain boundary regions so that the grain boundaries act as an extrinsic source of impedance. In many cases, double (back-to-back) Schottky potential barriers are created at interfaces between *n*-type grains due to charge trapping at acceptor states, resulting in bending of the conduction band across the grain boundary. This band bending produces an effective potential barrier of height, Φ_b, and depletion width, w, for conduction electrons between the grain and grain boundary regions, Fig. 2(a). The barrier can typically be characterized as a grain boundary impedance since it is both resistive (in comparison to the bulk) and of high capacitance due to the thin width of the depletion region with respect to the grain size.

In the absence of a dc bias, Φ_b is given by Eq. (1)

$$\Phi_b = \frac{qN_s^2}{8\varepsilon_0\varepsilon' N_d}, \tag{1}$$

where q is the electronic charge, N_s is the acceptor (surface charge) concentration, $\varepsilon_0 = 8.854 \times 10^{-14}$ F cm^{-1}, ε' is the

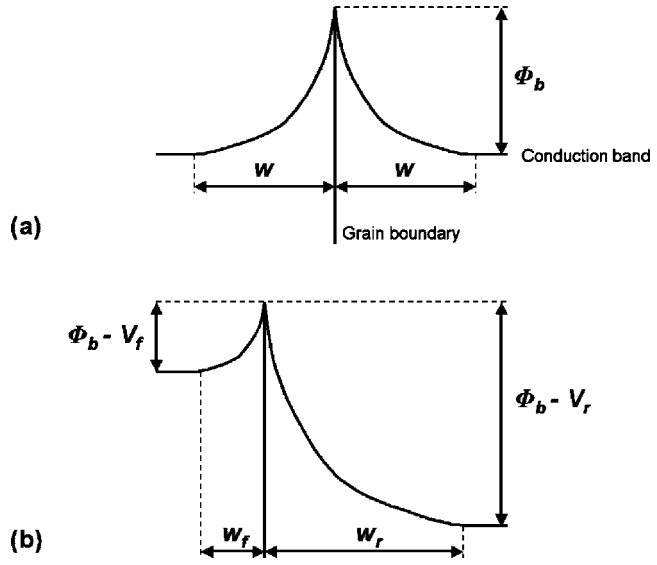

FIG. 2. Illustration of a back-to-back double Schottky barrier at a single grain boundary when (a) $V=0$ and (b) $V>0$.

permittivity of the material and N_d is the charge carrier concentration in the grains.[12] The depletion width on either side of the interface is identical and is proportional to barrier height, Φ_b, Eq. (2)

$$w = \left(\frac{2\Phi_b \varepsilon'}{qN_d}\right)^{1/2}. \tag{2}$$

This situation is shown schematically in Fig. 2(a). The grain boundary capacitance per unit area, in the absence of a dc bias, is given by

$$C_0 = \left(\frac{\varepsilon' qN_d}{8\Phi_b}\right)^{1/2}. \tag{3}$$

Given that CCTO is not ferroelectric[7] ($\varepsilon' < 100$ and shows little temperature dependence) the potential barrier height, Eq. (1), should show little temperature dependence assuming that N_d and N_s are relatively temperature independent at modest temperatures. The grain boundary conductivity, σ_{gb} (where $\sigma_{gb}=1/R_{gb}$) in the absence of a dc bias, is given by $\sigma_{gb}=A\exp(-\Phi_b/kT)$ where k=Boltzmann's constant and T=temperature.

Under a dc bias, V, the barrier becomes asymmetric such that the depletion width in the reverse direction, w_r, increases whereas the depletion width in the forward direction, w_f, decreases according to Eqs. (4) and (5), respectively, Fig. 2(b)

$$w_r = \left(\frac{\varepsilon'}{qN_d}\right)^{1/2} (\sqrt{4\Phi_b^2 + V^2} - V)^{1/2}, \tag{4}$$

$$w_f = \left(\frac{\varepsilon'}{qN_d}\right)^{1/2} (\sqrt{4\Phi_b^2 + V^2} + V)^{1/2}. \tag{5}$$

Mukae, Tsuda, and Nagasawa[13] have shown that the dependence of the grain boundary capacitance associated with the depletion region under a dc bias can be described by

$$\left(\frac{1}{C} - \frac{1}{2C_0}\right)^2 = \frac{2}{(\varepsilon' qN_d)}(\Phi_b + V), \tag{6}$$

where C is the biased grain boundary capacitance per unit area.

For a sufficiently large dc bias that there is a significant voltage drop across each grain boundary, C_{gb} decreases with increasing dc bias and a linear relation should be observed for a plot of $(1/C-1/2C_0)^2$ vs V with gradient related to Φ_b. Such voltage-dependent C_{gb} behavior has been reported for $BaTiO_3$-based ptcr thermistors;[14] the potential barrier height was in the range 0.4–0.8 V/grain boundary depending on temperature, since Φ_b varies significantly with temperature for ferroelectric $BaTiO_3$. As $R_b \ll R_{gb}$ in CCTO,[8] nearly all of the voltage drop occurs across the grain boundary regions, and R_{gb} decreases with increasing bias, Fig. 2(b). It is only the reduced barrier height that is observed in the IS response.

A common assumption for electrical property measurements of IBLC-like electrical microstructures is that, provided the data are corrected for sample geometry (i.e., pellet thickness and cross sectional area of the electrodes), the electrical properties should be independent of pellet thickness. For fine-grained ceramics, the change in number of grain boundaries on "thinning" a pellet by a factor of ~2–5 is usually not large enough to have any noticeable impact on geometry-corrected data and therefore the assumption holds true. If sample thickness is comparable to the grain size, however, then the change in number of grain boundaries as a function of pellet thickness can become significant and the electrical properties may vary significantly with pellet thickness. In the extreme case for large-grained ceramics, there may be no grain boundaries parallel to the electrodes after reducing the pellet thickness and the only source of impedance would be the semiconducting bulk material. In practice, ceramics often have a distribution of grain sizes which can be bi-modal with both large and small grains. In the latter case, current detours within the ceramic arise as the current avoids the fine-grained regions due to the high impedance associated with the high density of grain boundaries in such regions. It is also worth noting that the influence of a dc bias is more dramatic for large-grained ceramics as, for a given dc bias, the voltage drop per grain boundary is larger compared to that for a fine-grained ceramic of equivalent thickness.

III. EXPERIMENT

Fine- and coarse-grained CCTO ceramics with average grain sizes of ~3–5 and ~100–300 μm, respectively, were prepared by sintering single-phase CCTO pellets in air at 1100 °C for 3 and 24 h, respectively, as described in more detail previously.[7]

For the electrode material experiment, Au electrodes were sputtered on each pellet face of a coarse-grained ceramic with a current of 20 mA for 8 min using an Emscope EM400 sputter coating unit. Impedance measurements were taken with an applied voltage of 100 mV using a Hewlett-Packard 4192A impedance analyzer over the frequency range 5 Hz–2 MHz at selected temperatures between room tem-

perature (RT) and ~100 °C. At each temperature, further impedance measurements were taken with a dc bias of, 5, 10, and 15 V. After measurement, the Au-sputtered electrodes were removed and replaced by InGa (60:40 mol ratio). Impedance measurements were again taken between RT and ~100 °C at 0, 5, 10, and 15 V dc. The InGa electrodes were then removed and replaced by Au-sputtered electrodes using the method described above. RT impedance measurements were taken from 0 to 15 V dc at 1 V intervals. The Au-sputtered electrodes were then removed, replaced by InGa electrodes and RT impedance measurements again taken between 0 and 15 V dc at 1 V intervals. This procedure was also repeated for experiments on fine-grained ceramics. All IS data were corrected for pellet geometry and ZVIEW 2 software was used for data analysis.

For the sample thickness experiments, InGa electrodes were applied to fine- and coarse-grained pellets of thickness ~1.5–2.0 mm and the RT impedance measured. The electrodes were then removed and the pellets thinned by polishing with SiC paper. The geometric correction factors were recalculated, InGa electrodes reapplied and the RT impedance remeasured. This process was repeated until the pellet thickness was reduced to ~0.3 mm.

IV. RESULTS

Powder x-ray diffraction data on 3 and 24 h pellets were fully indexed on literature data,[1] showing all samples to be single-phase CCTO within the detection limits of laboratory x-ray diffraction. Scanning electron microscopy (SEM) micrographs of the 3 and 24 h CCTO ceramics are shown in Fig. 3. The 3 h sample exhibits a reasonably uniform microstructure with an average grain size of ~5 μm, whereas the 24 h sample exhibits exaggerated grain growth and a duplex microstructure consisting of very large grains in excess of 100 μm in length and isolated regions of fine grains (<10 μm).

The electrical results are subdivided into three sections: electrode materials, dc bias and sample thickness.

A. Electrode materials

Typical Z^* plots for a coarse-grained ceramic with Au-sputtered and InGa electrodes at ~85 °C are shown in Fig. 4(a). The data can be interpreted using the equivalent circuit in Fig. 1(a) and show R_{gb} and R_b [inset in Fig. 4(a)] to have values of ~45–50 kΩ and ~20 Ω, respectively, independent of the electrode material. In both cases, C_{gb} ~ 22 nF using the relationship $\omega RC=1$ at the arc maximum. This temperature, ~85 °C, is chosen to illustrate typical IS data, as the low frequency arc maximum associated with the grain boundary response for this sample was below the lower limit of the impedance analyzer at RT. Real capacitance, C', versus frequency for the same data is plotted in Fig. 4(b). Based on the interpretation reported previously, the high capacitance plateau in the kHz region corresponds to a grain boundary capacitance of ~15–22 nF, and the dispersion in the MHz region signifies relaxation of the grain boundary impedance to give data dominated by the conducting grains.

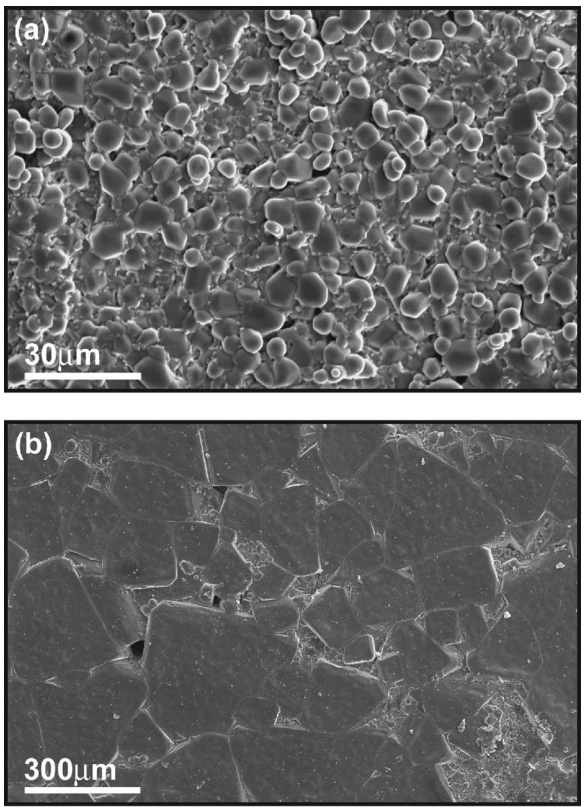

FIG. 3. SEM micrographs of CCTO ceramics sintered at 1100 °C in air for 3 h (a) and 24 h (b).

Data collected with InGa electrodes are nearly identical to those collected using Au electrodes.

Arrhenius plots of R_b^{-1} and R_{gb}^{-1} against temperature for the two different electrode materials are shown in Fig. 5 and reveal excellent agreement for R_b and R_{gb} over the measured temperature range. In both cases, the activation energies for bulk and grain boundary conduction are 0.06(2) and 0.66(2) eV, respectively.

B. DC bias

Typical Z^* plots for a coarse-grained ceramic with Au-sputtered electrodes at 86 °C with a dc bias of 0, 5 and 10 V are shown in Fig. 6(a). R_{gb} decreases dramatically with increasing dc bias from 43 kΩ with no dc bias to 10 kΩ at 10 V, whereas R_b ~ 20 Ω and is independent of the dc bias. The corresponding M'' spectroscopic plots show the Debye peak height associated with the grain boundary response to increase slightly with increasing dc bias, Fig. 6(b), indicating that C_{gb} decreases with increasing bias.

The voltage dependence of R_b, R_{gb}, and C_{gb} at RT for the same coarse-grained sample is shown in Figs. 7(a) and 7(b), respectively. R_b ~ 20 Ω and is independent of the dc bias, whereas R_{gb} displays an exponential decrease with increasing bias: the filled line represents a least squares fit to the $\ln R_{gb}$ against V data with an agreement factor (R^2) of >0.99, Fig. 7(a). C_{gb} was determined from M^* plots and shows a decrease from ~42 nF at 2 V dc to a near constant value of ~35 nF at 15 V dc, Fig. 7(b). A plot of $(1/C-1/2C_0)^2$ vs dc

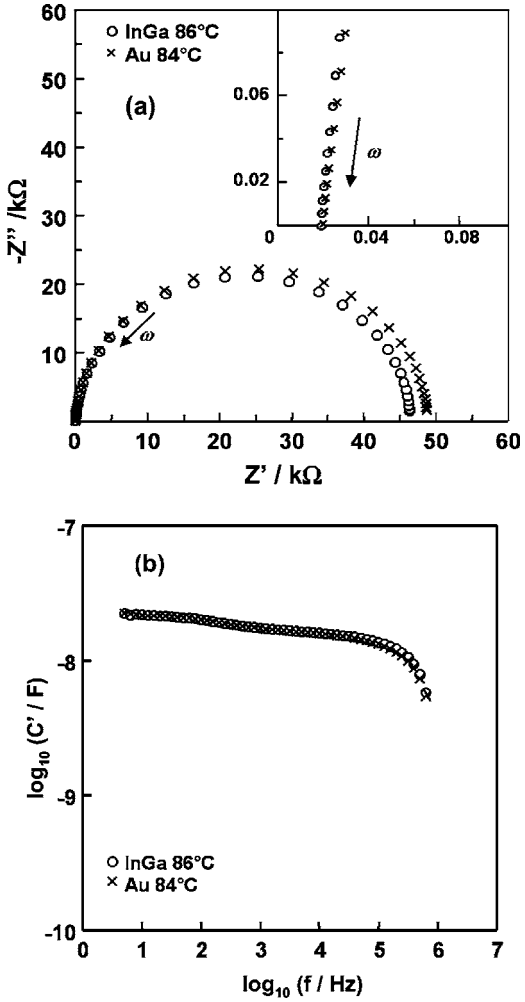

FIG. 4. Z^* plot (~85 °C) of a coarse-grained CCTO ceramic with InGa electrodes and Au electrodes (a) and corresponding C' spectroscopic plot (b).

bias per grain boundary shows excellent correlation with Eq. (6) and $\Phi_b \sim 0.77$ eV, Fig. 8.

Arrhenius plots of R_{gb}^{-1} against temperature for 0, 5, 10, and 15 V dc bias show the grain boundary resistance to decrease systematically with increasing bias and the activation energy to decrease from 0.66(2) eV with no dc bias to 0.46(2) eV at 15 V dc bias, Fig. 9.

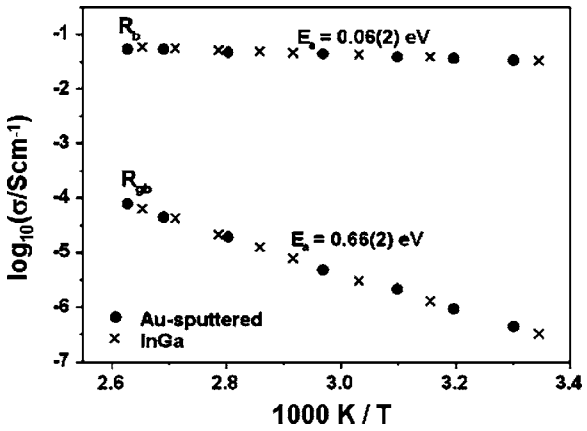

FIG. 5. Arrhenius plot of bulk and grain boundary conductivity data vs temperature for CCTO ceramics with InGa and Au electrodes.

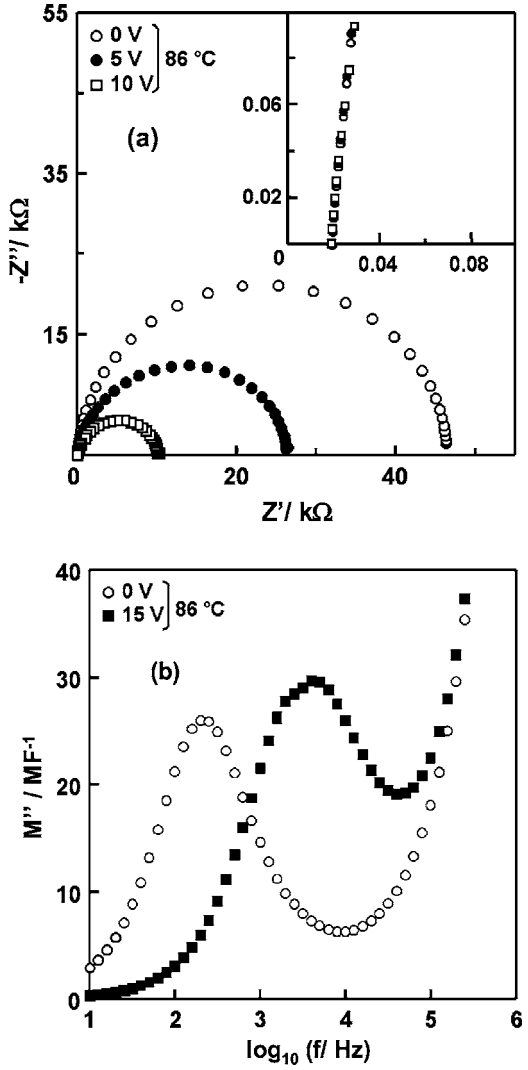

FIG. 6. Z^* plot of data obtained for a coarse-grained CCTO ceramic with a dc bias of 0 and 15 V (a) and corresponding M'' spectroscopic plots (b).

In contrast to Fig. 7(a), fine-grained ceramics displayed very weak voltage dependence at RT, Fig. 10. For example, R_{gb} decreased from ~4 MΩ (no dc bias) to ~2.5 MΩ at 4 V and remained constant up to 15 V dc. Similarly, no detectable change was observed in C_{gb} from M'' spectra or M^* plots as a function of dc bias.

C. Sample thickness

A coarse-grained ceramic of initial thickness ~1.9 mm with $R_{gb} \sim 4$ MΩ, $R_b \sim 25$ Ω, and $C_{gb} \sim 17.5$ nF at RT was polished to a thickness of ~0.6 mm, giving a slight decrease in R_{gb} to ~1.6 MΩ, an increase in C_{gb} to ~25 nF but no significant change in R_b, Fig. 11(a). Polishing to ~0.4 mm had a dramatic influence: R_{gb} decreased by nearly two orders of magnitude to ~32 kΩ and C_{gb} increased to ~27 nf. For a final pellet thickness of ~0.34 mm,

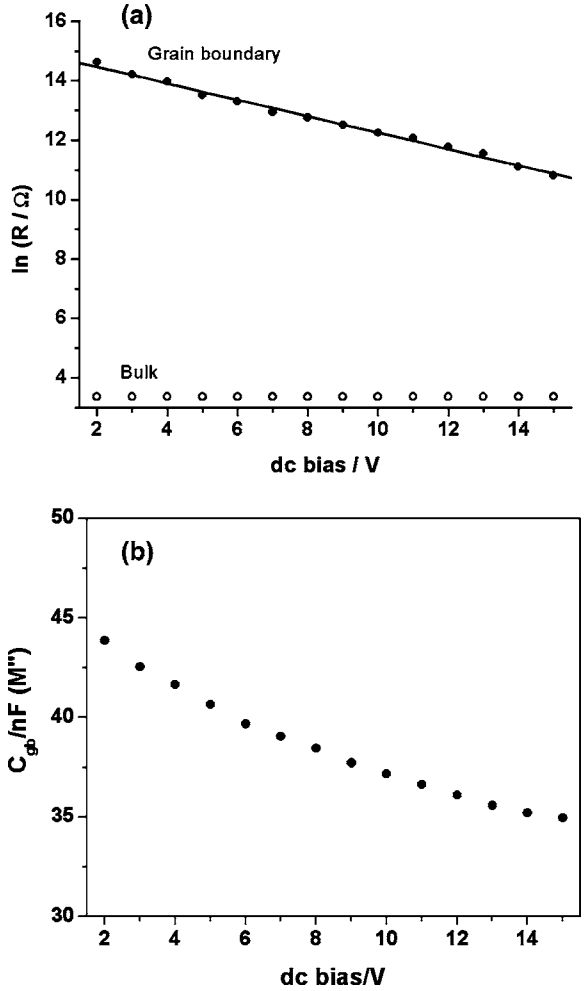

FIG. 7. R_{gb} and R_b vs dc bias (a) and C_{gb} vs dc bias (b) for a coarse-grained CCTO ceramic. Note: below a dc bias of 2 V it was not possible to observe the arc maximum in the Z^* plot (and therefore the corresponding Debye peak maximum in the M'' spectroscopic plots) as it occurred below the lower frequency limit of the impedance analyzer, therefore data for R_{gb} and C_{gb} are restricted to dc bias $\geqslant$2 V.

$R_{gb} \sim 25$ kΩ, $R_b \sim 40$ Ω, and $C_{gb} \sim 27$ nF, Fig. 11(a). It is worth noting that the time constant for the grain boundary response, τ_{gb}, where $\tau_{gb}=R_{gb}C_{gb}$ was $\sim$0.03 s and remained constant for thickness $>$0.55 mm. Below 0.5 mm, however, a significant decrease in τ_{gb} was observed to 0.005 s for $t<0.4$ mm.

In contrast, fine-grained ceramics displayed negligible variation with pellet thickness, Fig. 11(b). A fine-grained ceramic of initial thickness $\sim$1.4 mm had $R_b \sim 80$ Ω, $R_{gb} \sim 4$ MΩ and $C_b \sim 0.98$ nF at RT. Polishing to a final pellet thickness of $\sim$0.3 mm reduced R_{gb} slightly to $\sim$2.5 MΩ, although R_b remained unchanged and no significant variation in C_{gb} was observed, Fig. 11(b). The grain boundary response τ_{gb} was 0.002 s and independent of thickness.

V. DISCUSSION

SEM micrographs of CCTO pellets sintered at 1100 °C in air for 3 and 24 h show the development of dense ceramics

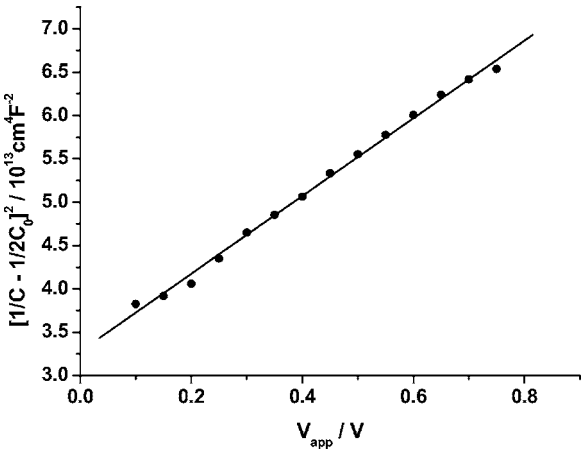

FIG. 8. $(1/C-1/2C_0)^2$ vs V for a coarse-grained CCTO ceramic. Note: The number of grain boundaries parallel to electrodes in this sample was estimated to be 20 (pellet $\sim$2 mm thick with an average grain size of $\sim$100 μm). The dc bias has been divided by 20 to give an x axis of applied voltage per grain boundary.

($\sim$95% of the theoretical x-ray density) with clear evidence of exaggerated grain growth for extended sintering periods of 24 h, Fig. 3. The grain growth mechanism is not currently understood but may be related to impurity contamination from the agate-based milling media and is under further investigation. All samples were phase pure by x-ray diffraction analysis, however, analytical electron microscopy is in progress to probe compositional variations within the grains/grain boundaries and will be reported elsewhere. For the present study, only the difference in grain size is considered in discussion of the electrical properties of CCTO ceramics.

All three experiments in this study provide evidence to support the IBLC-type model as the origin of the high effective permittivity in CCTO ceramics. The electrode material experiment was designed to test the influence of electrodes with significantly different electron work functions, i.e., Au (5.1 eV) and In:Ga alloy (4.1 eV), on the electrical response of CCTO ceramics. It is well known that nonohmic contacts can occur in n-type semiconducting titanates due to a mis-

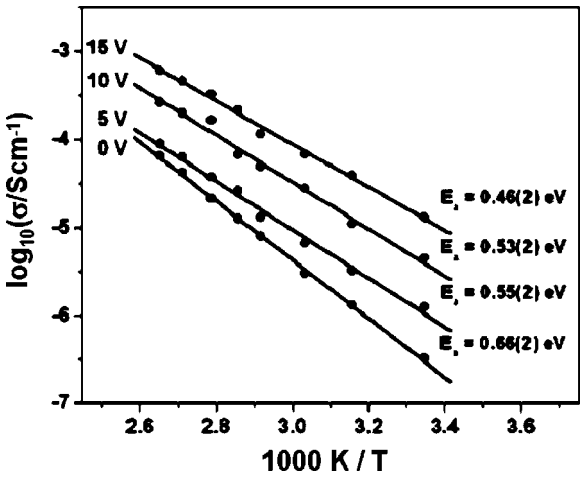

FIG. 9. Arrhenius plots of grain boundary conductivity as a function of dc bias for coarse-grained CCTO ceramics.

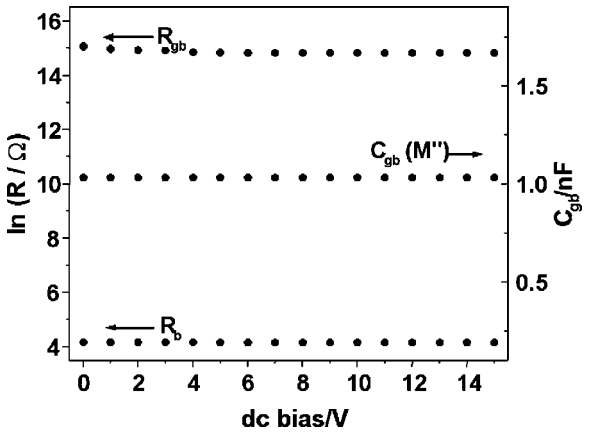

FIG. 10. Variation of R_{gb}, C_{gb} and R_b for a fine-grained CCTO ceramic as a function of dc bias.

match in the Fermi energy levels of the oxide and the metal. In particular, Au with a high electron work function can produce nonohmic contacts and can lead to an "additional" arc at low frequencies in Z^* plots and increased capacitance at low frequencies in spectroscopic plots of C'. In contrast, In:Ga alloy tends to give ohmic contacts to *n*-type semiconducting titanates, for example, ptcr-$BaTiO_3$ thermistors, and low frequency effects in addition to the grain boundary response are generally not observed.

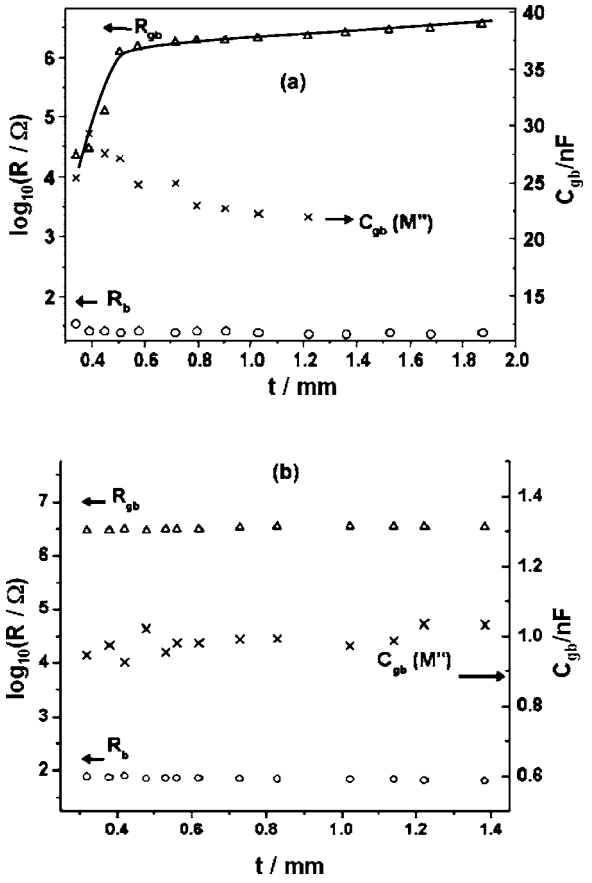

FIG. 11. R_{gb}, R_b and C_{gb} as a function of pellet thickness for coarse- and fine-grained CCTO ceramics (a) and (b), respectively.

The Z^* plots and C' spectroscopic plots in Fig. 4 for Au and In:Ga electrodes on CCTO ceramics show essentially the same response and both the magnitude of R_b and R_{gb} and the associated activation energies for the conduction processes are in excellent agreement over the measured temperature range irrespective of the electrode material, Fig. 5. The electrical response of CCTO ceramics does not show any significant variation with the work function of the electrode material, at least for Au and In:Ga alloy; thus, either both types of electrodes give ohmic contacts and the low frequency behavior is correctly assigned to the grain boundary response, or alternatively, both electrode types give rise to nonohmic contacts and the low frequency arc in Z^* plots and the high capacitance plateau in C' spectroscopic plots have been incorrectly identified as a grain boundary response, as suggested by Lunkenheimer *et al.*[11]

Although this experiment is not fully conclusive, the results from the dc bias and thickness experiments are difficult to explain using the nonohmic contact model. In particular, a nonohmic contact model would predict the same dc bias behavior for the low frequency arc in Z^* plots irrespective of the ceramic microstructure and this is clearly not the case, Figs. 7 and 10; it cannot explain why the low frequency arc in Z^* plots for coarse-grained samples shows a thickness dependence, whereas no variation with sample thickness is observed for fine-grained ceramics, Fig. 11. These results are discussed in more detail below where we conclude that the large low frequency arc in Z^* plots and the high capacitance plateau in C' spectroscopic plots is attributable primarily to a grain boundary response instead of a nonohmic electrode contact. There may be some nonohmic behavior associated with metal electrodes of different work function, however, it is difficult to detect in the presence of the dominant grain boundary response. It is worth noting that Schottky-type grain boundaries in CCTO ceramics have been observed directly by Chung *et al.*[9] using Kelvin probe microscopy, giving further credence to our interpretation of the IS results. It is appropriate to acknowledge that the work function of the metal electrode is not the only factor which governs the electrode contact conditions and that surface roughness[15] and wetting[16] are also important factors to consider when studying the influence of electrode contacts to functional oxides.

The results for the dc bias experiment depend on the ceramic microstructure and can be explained using an IBLC model and the effect of the electric field across individual grain boundaries in fine- and coarse-grained ceramics. The average grain size in the 3 h pellets is ~ 5 μm, which corresponds to ~ 400 grain boundaries parallel to the electrodes for a pellet of 2 mm thickness assuming an ideal brickwork layer model. For the 24 h pellets, the microstructure is very inhomogeneous with extremely large grains, $\sim 100-300$ μm and "islands" of fine grains, <10 μm in size. Assuming an average grain size of ~ 100 μm in the 24 h pellets, this corresponds to ~ 20 grain boundaries parallel to the electrodes for a pellet of 2 mm thickness. Although this is a highly simplified approximation, it is clear that the fine-grained ceramics have at least 20 times more grain boundaries than coarse-grained ceramics of equivalent thickness. On this basis, the electric field across each grain boundary in the fine-grained ceramics is considerably less than in coarse-grained ceramics for an equivalent dc bias.

The maximum bias in the impedance analyzer was restricted to 15 V and this corresponds to a maximum electric field of ~0.0375 and 0.75 V/grain boundary for the fine- and coarse-grained ceramics, respectively. The dc bias dependence of R_{gb} and C_{gb} for coarse-grained ceramics, Figs. 6 and 7, can therefore be attributed to the much higher electric field experienced by the grain boundaries in these samples. This is consistent with the expectation of a Schottky barrier model for the grain boundary with a reduction in potential barrier height in the forward bias direction and an increase in width of the depletion region, Fig. 2(b). As expected, since $R_b \ll R_{gb}$, R_b is independent of dc bias, Fig. 7(a). The dc bias behavior of C_{gb} shows excellent agreement with Eq. (6), as shown by the linear response in Fig. 8. In addition, the potential barrier height estimated from the dc bias dependence at RT is ~0.77 eV in reasonable agreement with the activation energy of ~0.66 eV obtained for the temperature dependence of grain boundary conduction, Fig. 5.

The influence of a dc bias on the temperature dependence of the grain boundary conductivity shown in Fig. 9 is also consistent with that expected from Schottky barrier behavior, viz., the dc bias reduces the potential barrier height in the forward bias direction and therefore the activation energy associated with the grain boundary conductivity decreases. The dc bias experiment demonstrates clearly that the grain boundary response is microstructure dependent, consistent with a Schottky barrier response and, therefore, CCTO ceramics display IBLC behavior.

The pellet thickness experiment reveals that it is possible to obtain very different results for the grain boundary response from IS depending on the ceramic microstructure and thickness of CCTO pellets, Fig. 11. Unfortunately, correction for the geometry of the grain boundaries cannot be made using standard impedance techniques and IS data are corrected only for the pellet geometry. The implication for CCTO ceramics is that the grain boundary impedance remains independent of thickness provided the pellet thickness is much greater than the grain size. This is the assumption made by Lunkenheimer *et al.*;[11] however, it is possible to obtain exaggerated grain growth in CCTO ceramics, Fig. 3(b), which results in large grain sizes in excess of 100 μm. As such a pellet is progressively thinned from an initial thickness of ~1.9 mm, the number of grain boundaries between the electrodes decreases rapidly with the result that the geometry "corrected" values of R_{gb} and C_{gb} appear to suddenly decrease and increase, respectively, at ~600 μm, Fig. 11. At the final pellet thickness of ~400 μm the number of grain boundaries has decreased rapidly and it may be that only one or two active grain boundaries exist between the electrodes. The slight variation in R_b and fluctuations in R_{gb} and C_{gb} are believed to be a consequence of inaccuracies in measuring the progressively smaller pellet dimensions and the heterogeneous nature of grain boundary geometry and composition.

The fine-grained sample exhibited no such trend in R_{gb} and C_{gb} since the typical grain size for these samples is ~1–10 μm and the final pellet thickness of ~400 μm remained ~ two orders of magnitude greater than the grain size. In this case, the number of grain boundaries per unit thickness would remain constant until the sample thickness became comparable with the average grain size of ~5 μm.

We observe that the change in τ_{gb} with pellet thickness for the coarse-grained pellets violates the brickwork layer model (BLM) used for analysis of the IS data and further investigations into τ_{gb} and its dependence on ceramic processing and electrical measurement parameters are in progress. The most likely explanation for the change in τ_{gb} is that the ceramic microstructure is nonuniform and results in an inhomogeneous field distribution and current detours at low frequencies. The BLM assumes cubic grains that are laterally homogeneous and that all grain boundaries are identical. Although this may seldom be the case in practice, providing the grain size is significantly smaller than the thickness of the pellet and there is not a large variation in the distribution of grain sizes and grain boundary composition, Fig. 3(a), this assumption holds reasonably well and IS is an appropriate method to characterize grain boundary behavior in electroceramics.

For coarse-grained ceramics, such as CCTO sintered for 24 h, Fig. 3(b), however, which contain regions of fine grains and regions of extremely large grains and where $R_b \ll R_{gb}$ the electrical current avoids the islands of fine grains due to the much higher number of grain boundaries in these regions and percolates preferentially through the large grains. Such an "electrical microstructure" has been simulated using finite element analysis by Fleig and Maier[17] whereby the magnitude of R_{gb} obtained from a low frequency arc in Z^* depends on the bulk conductivity, i.e., current detours around so-called "hindrances" (island of small grains) are easy for materials with high bulk conductivity. R_{gb} depends, therefore, not only on the spatial distribution of large- and fine-grained regions within the ceramic but also on the conductivity of both the grain and grain boundary phases.

The dependence of the low frequency data on the ceramic microstructure and pellet thickness may explain the wide variation in high effective permittivity values reported in the literature for CCTO ceramics and may also explain the pellet thickness-dependent results of Lunkenheimer *et al.*[11] In addition, the dc bias results demonstrate that commercial applications of CCTO-based ceramics as high voltage capacitor materials will require close control of the ceramic microstructure. Although large- or coarse-grained CCTO ceramics provide a high "effective" permittivity, such microstructures have much lower breakdown voltages compared to fine-grained CCTO ceramics. Further work is required to modify the chemical composition and ceramic processing of CCTO-based ceramics to optimize the bulk and grain boundary impedances to produce commercially viable IBLC-type devices.

VI. CONCLUSIONS

The low frequency IS response of CCTO ceramics appears to be independent of the electron work function of the metal electrode but shows a significant dependence on the ceramic microstructure. R_{gb} and C_{gb} values from the low frequency arc in Z^* plots for coarse-grained ceramics display significant variation with an applied dc bias and with pellet thickness, whereas no such effects are observed for fine-

grained ceramics. The voltage dependence of R_{gb} and C_{gb} for the coarse-grained ceramics is consistent with that expected from Schottky barrier behavior, with a potential barrier height of ~0.77 eV which is in good agreement with the value of ~0.66 eV obtained from the temperature dependence of R_{gb}. These results support the IBLC mechanism for the electrical behavior of CCTO ceramics, i.e., nonlinear *I-V* characteristics[10] and high effective permittivity values at radio frequencies,[4–8] as reported by various other groups in favor of an electrode-sample interface effect as reported recently by Lunkenheimer *et al.*[11]

The present work has concentrated on the influence of ceramic microstructure on the electrical properties of CCTO ceramics. Although this has been shown to be a very influential parameter, more information on the defect chemistry of CCTO and the composition of the grain boundary regions is required to understand the origin of the semiconductivity of the grains and the resistivity of the grain boundaries. This should allow better control of the potential barrier height in CCTO ceramics.

ACKNOWLEDGMENT

We thank the EPSRC for funding.

[1] A. Deschanvres, B. Raveau, and M. Tollermer, Bull. Soc. Chim. Fr. **11**, 4077 (1967).
[2] A. M. Glazer, Acta Crystallogr., Sect. B: Struct. Crystallogr. Cryst. Chem. **28**, 3384 (1972).
[3] S. M. Moussa and B. J. Kennedy, Mater. Res. Bull. **36**, 2525 (2001).
[4] M. A. Subramanian, D. Li, N. Duan, B. A. Reisner, and A. W. Sleight, J. Solid State Chem. **151**, 323 (2000).
[5] C. C. Holmes, T. Vogt, S. M. Sharpiro, S. Wakimoto, and A. P. Ramirez, Science **293**, 637 (2001).
[6] A. P. Ramirez, M. A. Subramanian, M. Gardel, G. Blumberg, D. Li, T. Vogt, and S. M. Shapiro, Solid State Commun. **115**, 217 (2000).
[7] D. C. Sinclair, T. B. Adams, F. D. Morrison, and A. R. West, Appl. Phys. Lett. **80**, 2153 (2002).
[8] T. B. Adams, D. C. Sinclair, and A. R. West, Adv. Mater. (Weinheim, Ger.) **14**, 1321 (2002).
[9] S. Y. Chung, I. L. D. Kim, and S. J. L. Kang, Nat. Mater. **3**, 774 (2004).
[10] R. K. Grubbs, E. L. Venturini, P. G. Clem, J. J. Richardson, B. A. Tuttle, and G. A. Samara, Phys. Rev. B **72**, 104111 (2005).
[11] P. Lunkenheimer, R. Fichtl, S. G. Ebbinghaus, and A. Loidl, Phys. Rev. B **70**, 172102 (2004).
[12] F. Greuter and G. Blatter, Semicond. Sci. Technol. **5**, 111 (1990).
[13] K. Mukae, K. Tsuda, and I. Nagasawa, J. Appl. Phys. **50**, 4475 (1979).
[14] Y. G. Li and S. G. Cho, J. Appl. Phys. **91**, 4535 (2002).
[15] R. de Levie, Electrochim. Acta **10**, 113 (1965).
[16] E. J. Abram, D. C. Sinclair, and A. R. West, J. Electroceram. **7**, 179 (2001).
[17] J. Fleig and J. Maier, J. Eur. Ceram. Soc. **19**, 693 (1999).